

Microscopic calculation of the form factors for deeply inelastic heavy-ion collisions within the statistical model

B. R. Barrett,*† S. Shlomo,‡ and H. A. Weidenmüller

Max-Planck-Institut für Kernphysik, Heidelberg, West Germany

(Received 7 September 1977)

Agassi, Ko, and Weidenmüller have recently developed a transport theory of deeply inelastic heavy-ion collisions based on a random-matrix model. In this work it was assumed that the reduced form factors, which couple the relative motion with the intrinsic excitation of either fragment, represent a Gaussian stochastic process with zero mean and a second moment characterized by a few parameters. In the present paper, we give a justification of the statistical assumptions of Agassi, Ko, and Weidenmüller and of the form of the second moment assumed in their work, and calculate the input parameters of their model for two cases: ^{40}Ar on ^{208}Pb and ^{40}Ar on ^{120}Sn . We find values for the strength, correlation length, and angular momentum dependence of the second moment, which are consistent with those estimated by Agassi, Ko, and Weidenmüller. We consider only inelastic excitations (no nucleon transfer) caused by the penetration of the single-particle potential well of the light ion into the mass distribution of the heavy one. This is combined with a random-matrix model for the high-lying excited states of the heavy ion. As a result we find formulas which relate simply to those of Agassi, Ko, and Weidenmüller, and which can be evaluated numerically, yielding the results mentioned above. Our results also indicate for which distances of closest approach the Agassi-Ko-Weidenmüller theory breaks down.

[NUCLEAR REACTIONS Random-matrix model and shell model used to calculate distribution of form factors.]

I. INTRODUCTION

A transport theory of deeply inelastic heavy-ion reactions based on a random-matrix model has recently been developed by Agassi, Ko, and Weidenmüller¹ (hereafter referred to as AKW). In this theory, the deeply inelastic collisions are essentially viewed as a sequence of a large number of distorted-wave Born approximation (DWBA) type excitations of either fragment. Each such individual excitation is characterized by a form factor, a quantity familiar from DWBA theory. This form factor couples relative motion with intrinsic excitation and is responsible for the transfer of energy and angular momentum from relative motion to intrinsic excitation. Because of the complexity of the highly excited states in either fragment, AKW used a random-matrix model to describe the statistical distribution of the form factors. It was assumed that the form factors are a Gaussian stochastic process with mean value zero and a second moment of simple form, characterized by a few parameters. Values for these parameters were also estimated by AKW. The assumptions just mentioned determine the form of the transport equation which in turn allows for a calculation of cross sections. Such calculations seem to yield encouraging agreement with the data.²

In view of these developments and results and in view of the fact that the entire AKW theory de-

pends somewhat critically on the input, i.e., on the assumptions used for the statistical properties of the form factors, a microscopic determination of this input is highly desirable, and forms the subject of the present investigation. If a sufficiently precise statement about the statistical properties of the form factors can be attained from a microscopic model, a comparison of the results of the AKW theory with the data should indicate whether the mechanism underlying the theory is, indeed, mainly responsible for the large energy loss observed, or whether other excitations of a collective type not considered in this theory play an equally important role. In this sense the present paper forms an integral part of a series of investigations aimed at unravelling the physical mechanism responsible for the deeply inelastic collisions.

In pursuing our goal—a microscopic calculation of the input of the AKW theory—we naturally use the same physical assumptions as AKW on the nature of the deeply inelastic collisions. In particular, we neglect surface deformations and other collective modes of excitation of either fragment. Aside from the remarks made in the previous paragraph, more about the underlying physical picture may be found in the Introduction and in Sec. 2 of Ref. 1. Moreover, we focus attention upon only one particular mode of excitation, i.e., creation of particle-hole pairs in one fragment by the single-particle potential of the other. We

thereby neglect nucleon exchange, probably the most important mechanism for mass exchange between the two fragments, and the contribution of genuine two-body nucleon-nucleon scattering (with one nucleon in either fragment being excited) to inelastic excitations. Concerning the former mechanism, we do not believe it to be unimportant, but rather view the present paper as a first step which should later be followed by a similar study of nucleon exchange processes. Concerning the latter, we do believe it to be less important than the mechanism studied here because of reduced overlap.

Our microscopic model is described in Sec. II where we also derive the expression for the form factors coupling relative motion with intrinsic excitation, and relate them to the formulas of AKW. Section III contains a description of our calculations, and of the results. In Sec. IV we discuss these results and compare them with the assumptions and estimations of AKW.

II. THEORY

A. Review of the assumptions of AKW

It is assumed that the deeply inelastic collision happens when the tails of the density distributions of the two fragments overlap. For this reason, an expansion in terms of the states $|sIM\rangle$ is used, which are products of the eigenstates of the two separated fragments, coupled to total spin I with z projection M . The form factors referred to in the Introduction are then defined by

$$V_{ss'}(\vec{R}) = \langle sIM | V_{\text{int}}(\vec{R}, \vec{\xi}_1, \vec{\xi}_2) | s'I'M' \rangle. \quad (1)$$

Here, $V_{\text{int}}(\vec{R}, \vec{\xi}_1, \vec{\xi}_2)$ is that part of the Hamiltonian which couples the coordinate \vec{R} of relative motion (the distance between the two centers of mass) with the intrinsic coordinates $\vec{\xi}_1$ and $\vec{\xi}_2$ of the two fragments. The form of V_{int} will be specified below. In the definition of the states $|sIM\rangle$ as product states and in that of the coordinate \vec{R} we have neglected antisymmetrization of nucleons in different fragments. For the nearly grazing collisions here considered, this should be a good approxima-

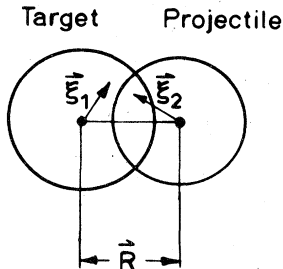


FIG. 1. Coordinates in the collision of two heavy ions.

tion. The geometrical significance of the variables \vec{R} , $\vec{\xi}_1$, and $\vec{\xi}_2$ is depicted in Fig. 1.

Expanding V_{int} into spherical harmonics with respect to \vec{R} and the intrinsic variables, and using the Wigner-Eckart theorem, we can write $V_{ss'}(\vec{R})$ in terms of the reduced form factors

$$(sI \| V_L [R] Y_L \| s'I')$$

as

$$V_{ss'}(\vec{R}) = \sum_{L=0}^{L_{\text{max}}} \sum_{\lambda} \frac{4\pi}{2L+1} Y_L^{*\lambda}(\hat{R}) (-)^{I-M} \begin{pmatrix} I & L & I' \\ -M & \lambda & M' \end{pmatrix} \times (sI \| V_L [R] Y_L \| s'I'). \quad (2)$$

The quantity $\hbar L$ signifies the angular momentum transfer per individual excitation. The sum over L has a natural cutoff at a maximum angular-momentum transfer $\hbar L_{\text{max}}$. For single-particle transitions from the last filled to the first unfilled shell in Pb, for example, we find $L_{\text{max}} \cong 12$.

The reduced form factors are assumed in AKW to represent a Gaussian stochastic process in $|\vec{R}|$ with mean value zero (for $s \neq s'$) and a second moment given by

$$\begin{aligned} & \langle (sI \| V_L [R] Y_L \| s'I') (s'I' \| V_{L'} [R'] Y_{L'} \| s''I'') \rangle_{\text{ave}} \\ &= (-)^{I-I'} (2I+1)^{1/2} (2I'+1)^{1/2} \frac{2L+1}{4\pi} \\ & \times \delta_{ss'} \delta_{II''} \delta_{LL'} \alpha_L(s, s'; I, I'; R, R'), \end{aligned} \quad (3)$$

where the $\langle \rangle_{\text{ave}}$ denotes the ensemble average, and where α_L is parametrized as

$$\begin{aligned} & \alpha_L(s, s'; I, I'; R, R') \\ &= \omega_L [\rho_I(s) \rho_{I'}(s')]^{-1/2} \\ & \times \exp[-(\epsilon_s - \epsilon_{s'})^2 / (2\Delta^2)] \\ & \times \exp[-(R - R')^2 / (2\sigma^2)] f(\frac{1}{2}(R + R')). \end{aligned} \quad (4)$$

In Eq. (4), ω_L is a strength factor with the dimension of energy, $\rho_I(s)$ is the joint mean level density of the two heavy ions at an excitation energy ϵ_s and for a spin I , and f is a dimensionless function which describes the overlap of the mass densities of the two heavy ions.

The assumption that the reduced form factors constitute a Gaussian ensemble is based on the statistical properties of the states $|sIM\rangle$ which, at sufficiently high excitation energies (≈ 5 MeV for heavy nuclei) are extremely complex. It will be shown below that this assumption as well as the assumption that the nondiagonal reduced form factors have zero mean are simple consequences of a random-matrix model for the states $|sIM\rangle$. The critical issue is thus to justify the detailed

form of the second moment given in Eqs. (3) and (4). It is from this form that numerical values for cross sections follow via the transport theory developed by AKW. In AKW, ω_L was assumed to be independent of L and of the order of magnitude of a few MeV, Δ was estimated to be 5 to 7 MeV, and the correlation length σ was estimated to be 1 to 2 fm in the interior region and larger at the surface, the domain of interest for deeply inelastic collisions.

B. A microscopic statistical model

In order to devise a microscopic model for the reduced form factors, we have to specify the nature of the interaction V_{int} , and we have to introduce a random-matrix model for the states $|sIM\rangle$. We describe these two steps in turn. Simple level-density arguments show that in a collision between a light ion of mass 40 or 60 and a heavy ion of mass 200, the overwhelming fraction of the excitation energy resides in the heavy ion. We therefore simplify the presentation by replacing the product states $|sIM\rangle$ by those of the heavy ion. The error incurred is expected to lie in the 10 to 20% region and is roughly consistent with the estimated overall accuracy of our deduction.

The interaction V_{int} is a sum of a one-body interaction (the mean field or average single-particle potential of the light ion penetrating into the mass distribution of the heavy one) and a two-body interaction (the residual two-body interaction between nucleons in different fragments giving rise to simultaneous particle-hole excitations in both fragments). Due to reduced overlap, we expect the matrix elements of the latter to be smaller by 1 or 2 orders of magnitude than those of the former, and we therefore consider only the one-body interaction. (The way in which the mutual interpretation of the single-particle potential of one heavy ion into the mass distribution of the other gives

rise to an ever increasing number of particle-hole excitations in both fragments is schematically illustrated in Fig. 2.)

To describe the action of the mean field of the light ion on the heavy one, hereafter referred to as fragment 1, we use a shell-model description for the states of the latter. In adopting a shell-model or single-particle model for fragment 1, and in replacing the set of intrinsic coordinates ξ_1 introduced above by the coordinates \vec{r}_i , $i=1, \dots, A_1$ of the A_1 independent particles of fragment 1, we run into the well-known center-of-mass problem. Since $1/A_1 \cong 0.5\%$, we disregard this problem. The coordinates \vec{r}_i refer to the center-of-mass of fragment A_1 as their origin, and V_{int} is a sum of A_1 terms, each depending on the variable $|\vec{R} - \vec{r}_i|$, $i=1, \dots, A_1$, where we use the spherical symmetry of the single-particle potential $V^{\text{s.p.}}$ generated by fragment 2 and neglect the spin-orbit term,

$$V_{\text{int}} = \sum_{i=1}^{A_1} V^{\text{s.p.}}(|\vec{R} - \vec{r}_i|). \quad (5)$$

Each term in the sum on the right hand side (rhs) of Eq. (5) can be expanded in terms of spherical harmonics. (Such an expansion is analytically feasible only if $V^{\text{s.p.}}$ is of sufficiently simple analytic form. We return to this point in Sec. III.) We write

$$V_{\text{int}} = \sum_{i=1}^{A_1} \sum_{L=0}^{\infty} \sum_{\lambda=L}^{+L} V_L^{\text{s.p.}}(|\vec{R}|, |\vec{r}_i|) Y_L^{\lambda}(\hat{R}) Y_L^{\lambda}(\hat{r}_i) \times \frac{4\pi}{2L+1}. \quad (6)$$

This defines the coefficients $V_L^{\text{s.p.}}$.

We now turn to the states $|sIM\rangle$. Because of the simplifications introduced in the first paragraph of this subsection, these are just the intrinsic eigenstates of fragment 1. We use a shell model to describe the excited states of fragment 1. We introduce the shell-model states Ψ_{α}^{IM} by coupling all particles not in closed shells to a total spin I and z projection M , paying proper attention to the exclusion principle. The label α distinguishes states with the same (I, M) . We expand the state $|sIM\rangle$ in terms of the complete set Ψ_{α}^{IM} ,

$$|sIM\rangle = \sum_{\alpha} A_{\alpha}^{sI} \Psi_{\alpha}^{IM}. \quad (7)$$

Because of time-reversal invariance, the phases can be chosen in such a way that the coefficients A_{α}^{sI} are real. They form the elements of an orthogonal matrix,

$$\sum_s A_{\alpha}^{sI} A_{\alpha'}^{sI} = \delta_{\alpha\alpha'}; \quad \sum_{\alpha} A_{\alpha}^{sI} A_{\alpha}^{s'I} = \delta_{ss'}. \quad (8)$$

The random-matrix model for the states $|sIM\rangle$

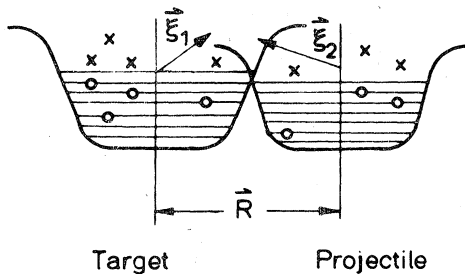


FIG. 2. Schematic representation of the way in which particle-hole excitations in both fragments are produced by the overlap of the two single-particle potential wells.

is introduced by assuming that the coefficients A_α^{sI} are random variables with a distribution to be specified below. Before this is done, we introduce another set of coefficients more appropriate for the evaluation of the form factors (1). Since by Eq. (5) V_{int} is a sum of one-body operators, it is useful to expand the states Ψ_α^{IM} into products of single-particle states ϕ_{nj}^μ characterized by radial quantum number n , orbital angular momentum l , and spin j , and of states χ_β^{JM} of $A_1 - 1$ particles constructed just like the states Ψ_α^{IM} themselves. This can be done by introducing formally generalized coefficients of fractional parentage (CFP) and yields

$$\begin{aligned} \Psi_\alpha^{IM}(1, \dots, A_1) \\ = \sum_{\beta n l j \mu} \{ \text{CFP}[\alpha I | \beta J; n l j] \} (JM - \mu j \mu | IM) \\ \times \phi_{nj}^\mu(A_1) \chi_\beta^{JM-\mu}(1, \dots, A_1 - 1). \end{aligned} \quad (9)$$

Here, $(JM - \mu j \mu | IM)$ is a usual Clebsch-Gordan coefficient. When the expansions (7) and (9) are used to calculate the form factors (1), only the product of the coefficients A_α^{sI} with the CFP appears. It is therefore convenient to define the coefficients

$$B_{\beta J; n l j}^{sI} = A_1^{1/2} \sum_{\alpha} A_\alpha^{sI} \{ \text{CFP}[\alpha I | \beta J; n l j] \}, \quad (10)$$

where we have introduced a factor $A_1^{1/2}$ in the definition. This factor just absorbs an overall factor A_1 which arises upon evaluation of the form factor from the sum in Eq. (5) and antisymmetry of the wave functions $|sIM\rangle$.

We now introduce the statistical model for the states $|sIM\rangle$ by assuming that the coefficients B of Eq. (10) are real random variables. From the study of the Gaussian orthogonal ensemble, it is known³ that expansion coefficients like the quantities A_α^{sI} have a Gaussian distribution with mean value zero and a diagonal second moment, and we shall assume this here also:

$$\begin{aligned} \langle A_\alpha^{sI} \rangle_{\text{ave}} &= 0, \\ \langle A_\alpha^{sI} A_{\alpha'}^{s'I'} \rangle_{\text{ave}} &= \delta_{II'} \delta_{ss'} \delta_{\alpha\alpha'} \langle |A_\alpha^{sI}|^2 \rangle_{\text{ave}}. \end{aligned} \quad (11)$$

The $\langle \rangle_{\text{ave}}$ denotes the ensemble average. It follows from Eq. (10) and the law of large numbers that the coefficients B also have a Gaussian distribution with mean value zero, and it remains to work out the second moment. This can be done only approximately and forms the content of the remainder of this subsection.

Using Eqs. (10, 11), we find

$$\begin{aligned} \langle B_{\beta J; n l j}^{sI} \rangle_{\text{ave}} &= 0; \\ \langle B_{\beta J; n l j}^{sI} B_{\beta' J'; n' l' j'}^{s'I'} \rangle_{\text{ave}} \\ &= \delta_{ss'} \delta_{II'} A_1 \\ &\times \sum_{\alpha} \langle |A_\alpha^{sI}|^2 \rangle_{\text{ave}} \{ \text{CFP}[\alpha I | \beta J; n l j] \} \\ &\times \{ \text{CFP}[\alpha I | \beta' J'; n' l' j'] \}. \end{aligned} \quad (12)$$

The product states $\phi_{nj}^\mu \chi_\beta^{JM}$ are not antisymmetric, and the CFP are therefore not the elements of an orthogonal transformation. If they were, it would be easy to argue that the second moment of the B 's is diagonal also in (β, β') , (JJ') , (nn') , (ll') , (jj') . Actually, this is not necessarily true. Being unable to evaluate the relation (12) in a more accurate way, we shall, nevertheless, make this assumption, relying on a cancellation of terms with opposite signs for the nondiagonal parts of the second moment,

$$\begin{aligned} \langle B_{\beta J; n l j}^{sI} B_{\beta' J'; n' l' j'}^{s'I'} \rangle_{\text{ave}} &= \delta_{ss'} \delta_{II'} \delta_{\beta\beta'} \delta_{JJ'} \delta_{nn'} \delta_{ll'} \delta_{jj'} \\ &\times \langle |B_{\beta J; n l j}^{sI}|^2 \rangle_{\text{ave}}. \end{aligned} \quad (13)$$

At this point the reader may wonder why we go through the trouble of working in a scheme with angular-momentum coupling rather than in the m scheme, where these problems would disappear. We do this in order to connect our work with the AKW formulas which relate to the reduced matrix elements. Use of the latter in AKW is indispensable for keeping proper track of the angular-momentum transfer from relative motion into intrinsic excitation. This transfer affects the angular distributions.

In order to evaluate the rhs of Eq. (13), we introduce a model, and thereby an approximation. We emphasize from the outset that because of reasons to be explained below, this approximation is accurate only to within a factor of 2 or so. We shall see, however, that the approximation mainly affects the strength factor of the second moment, i.e., the quantity denoted by ω_L in Eq. (4), while it has little influence on the other factors on the rhs of Eq. (4) and virtually none on the radius-dependent quantities appearing there.

We assume that fragment 1 is doubly magic. This simplifies the presentation but does not affect the generality of our results. We specify the label β introduced in Eq. (9) by two new labels, N and γ . Here, N denotes the number of particles above the Fermi surface, and γ is a further label needed to specify the states completely. For later use we observe that the number of holes in the state β is $(N+1)$. This is because the states labeled α have equal numbers of particles and holes.

The model for the rhs of Eq. (13) consists in assum-

ing that the state $|sIM\rangle$ is spread over the angular momentum coupled product states $\{\phi_{nlj}\chi_{sIM}^j\}$ (or, conversely, that each such product state is spread over the states $|sIM\rangle$) in a manner known for isolated doorway states and given essentially by a Lorentzian. To make this statement more precise, we introduce a few definitions. Let $\epsilon_{N\gamma J}$ be the excitation energy of the states $\chi_{N\gamma}^j$, and let $\rho_{N\gamma}^{A-1}(\epsilon_{N\gamma J})$ be their mean level density, $D_{N\gamma}^{A-1} = (\rho_{N\gamma}^{A-1})^{-1}$ their mean level spacing. The index $(A-1)$ is introduced to recall that these states refer to the $(A-1)$ particle system. (To simplify the formulas, we replace A_1 by A in the sequel.) Similarly, let ϵ_{nlj} be the single-particle energy, which is larger (smaller) than the Fermi energy ϵ_F for particles (holes), and let $\bar{\epsilon}_{nlj} = |\epsilon_F - \epsilon_{nlj}|$ be the excitation energy of such a state, with $\rho_{lj}^1(\bar{\epsilon}_{nlj})$ the associated level density. Throughout our work, we disregard the spin-orbit splitting and therefore suppress the index j of ϵ_{nlj} and ρ_{lj}^1 in the sequel. We also assume that the densities of particles and holes summed over l and j are about the same near the Fermi surface. It then

follows that

$$\sum_{i,J} \int d\bar{\epsilon}_{nl} \int d\epsilon_{N\gamma J} \delta(\bar{\epsilon}_{nl} + \epsilon_{N\gamma J} - E) \times \rho_i^1(\bar{\epsilon}_{nl}) \rho_{N\gamma}^{A-1}(\epsilon_{N\gamma J}) \theta(\epsilon_F - \epsilon_{nl}) = \rho_{NI}^A(E) \quad (14a)$$

and

$$\sum_{i,J} \int d\bar{\epsilon}_{nl} \int d\epsilon_{N\gamma J} \delta(\bar{\epsilon}_{nl} + \epsilon_{N\gamma J} - E) \times \rho_i^1(\bar{\epsilon}_{nl}) \rho_{N\gamma}^{A-1} \theta(\epsilon_{nl} - \epsilon_F) = \rho_{N+1I}^A(E). \quad (14b)$$

We denote by $P_{NI}^A(\epsilon)$ the probability of finding a state with N particles and holes and spin I at energy ϵ . Obviously, we have

$$D_I^A(\epsilon) = D_{NI}^A(\epsilon) P_{NI}^A(\epsilon), \quad (15)$$

where $D_I^A(\epsilon)$ is the mean level spacing of all the states with spin I at excitation energy ϵ . The parametrization for the second moment of the B^j 's is written in the form

$$\langle |B_{N\gamma J;nlj}^{sI}|^2 \rangle_{\text{ave}} = \left[\frac{1}{2} \theta(\epsilon_F - \epsilon_{nl}) P_{NI}^A(\epsilon_s) D_{NI}^A(\bar{\epsilon}_{nl} + \epsilon_{N\gamma J}) + \frac{1}{2} \theta(\epsilon_{nl} - \epsilon_F) P_{N+1I}^A(\epsilon_s) D_{N+1I}^A(\bar{\epsilon}_{nl} + \epsilon_{N\gamma J}) \right] \times \frac{\Gamma/(2\pi)}{(\epsilon_s - \bar{\epsilon}_{nl} - \epsilon_{N\gamma J})^2 + \frac{1}{4} \Gamma^2}. \quad (16)$$

The quantity Γ denotes a spreading width which we estimate to be 5 to 10 MeV, a value typical for spreading widths of states at excitation energies of 20 or 40 MeV. The physical interpretation of Eq. (16) is straightforward. The last factor describes the Lorentzian spread referred to above. The factor in square brackets distinguishes the case $\epsilon_F > \epsilon_{nl}$, when the product state contains N particles and holes, and $\epsilon_F < \epsilon_{nl}$, when the product state contains $(N+1)$ particles and holes. The factors D_{NI}^A are necessary for dimensional reasons and in order to ensure proper normalization. To see this, we notice that the coefficients B must obey the relations

$$\sum_{N\gamma J;nlj} \langle |B_{N\gamma J;nlj}^{sI}|^2 \rangle_{\text{ave}} = 1$$

and

$$\sum_s \langle |B_{N\gamma J;nlj}^{sI}|^2 \rangle_{\text{ave}} = 1. \quad (17)$$

Equations (17) hold if we assume the CFP's to be approximately orthogonal, as we did in Eq. (13). To check the first of Eqs. (17), we use Eq. (16) and sum it over the relevant indices. We change the summations into integrations, putting in the appropriate level densities, and use Eq. (14). Ob-

serving that $\sum_N P_{NI}^A(\epsilon) = 1$ for all ϵ , we see that the first of Eqs. (17) is fulfilled. It is instructive to check also the second of these equations. Starting again from Eq. (16) and changing the summation into an integration, we immediately find the desired result if we replace the argument $(\bar{\epsilon}_{nl} + \epsilon_{N\gamma J})$ of D_N and D_{N+1} by ϵ_s and use the relation (15).

The substitution $\bar{\epsilon}_{nl} + \epsilon_{N\gamma J} \rightarrow \epsilon_s$ is justified only if the ratio $D_{NI}(\bar{\epsilon}_{nl} + \epsilon_{N\gamma J})/D_{NI}(\epsilon_s)$ is sufficiently close to unity over the range of the ϵ_s integration. Because of the exponential dependence of D_N on ϵ_s , and the very slow rate of change of the Lorentzian, this substitution is never really justified. We disregard this problem since an attempt to improve on the formula (16) would involve a considerable amount of analytical work. This seems hardly worthwhile since so little is known about the details of formulas like (16). We prefer to view Eq. (16) as a rough approximation. Wherever necessary, we shall stipulate that the Lorentzian falls off more strongly than the level density changes, although this is analytically not so. As remarked above, this procedure will be seen to influence mainly the strength ω_L of the second moment, but not the other factors.

In the light of these remarks, we may introduce

the substitution $\bar{\epsilon}_{nl} + \epsilon_{N\gamma J} - \epsilon_s$ from the outset in Eq. (16). Together with Eq. (15), this leads to the simple expression

$$\langle B_{N\gamma J;nlj}^{sI} |^2 \rangle_{\text{ave}} = D_I^A(\epsilon_s) \frac{\Gamma/(2\pi)}{(\epsilon_s - \bar{\epsilon}_{nl} - \epsilon_{N\gamma J})^2 + \frac{1}{4}\Gamma^2}. \quad (18)$$

This is the form of $|B|^2$ we shall use henceforth. It obviates the necessity to introduce the quantities D_{NI} , P_{NI} defined above. We have, nevertheless, preferred to use the apparent detour via Eq. (16) to exhibit the type of approximation we

shall use throughout. We hope that this will convey a better feeling for the limitations of our estimations than a straightforward presentation proceeding directly via Eq. (18) would have conveyed.

C. Distribution of form factors

With the help of the formulas of Sec. II B, we can now determine the distribution of the form factors (1). Using Eqs. (6), (7), (9), and (10) in Eq. (1), we find after some straightforward angular-momentum algebra

$$\begin{aligned} \langle sIM | V_{\text{int}} | s'I'M \rangle &= \sum_{N\gamma Jnljn'l'j'} B_{N\gamma J;nlj}^{sI} B_{N\gamma J;n'l'j'}^{s'I'} \sum_{I=0}^{\infty} \sum_{\lambda=-L}^{+L} (-)^{1/2-J-I'} \frac{4\pi}{2L+1} \\ &\times [2l+1)(2l'+1)(2j+1)(2j'+1)(2I+1)(2I'+1)(2L+1)/(4\pi)]^{1/2} \\ &+ \begin{pmatrix} l & L & l' \\ 0 & 0 & 0 \end{pmatrix} \begin{Bmatrix} l & j & \frac{1}{2} \\ j' & l' & L \end{Bmatrix} \begin{Bmatrix} L & j' & j \\ J & I & I' \end{Bmatrix} (R_{nl} | V_L^{\text{s.p.}} | R_{n'l'}) Y_L^{\lambda}(\hat{R}) (-)^{I-I'} \begin{pmatrix} I & L & I' \\ -M & \lambda & M' \end{pmatrix}. \quad (19) \end{aligned}$$

Here, R_{nl} is the radial part of the single-particle wave function ϕ_{nlj}^{μ} . Comparing this with the AKW result, Eq. (2), we find that the reduced form factors are given by

$$\begin{aligned} (sI || V_L Y_L || s'I') &= \sum_{N\gamma Jnljn'l'j'} B_{N\gamma J;nlj}^{sI} B_{N\gamma J;n'l'j'}^{s'I'} \\ &\times (-)^{1/2-J-I} [(2l+1)(2l'+1)(2j+1)(2j'+1)(2I+1)(2I'+1)(2L+1)/(4\pi)]^{1/2} \\ &\times \begin{pmatrix} l & L & l' \\ 0 & 0 & 0 \end{pmatrix} \begin{Bmatrix} l & j & \frac{1}{2} \\ j' & l' & L \end{Bmatrix} \begin{Bmatrix} L & j' & j \\ J & I & I' \end{Bmatrix} (R_{nl} | V_L^{\text{s.p.}} | R_{n'l'}). \quad (20) \end{aligned}$$

In view of the fact that the rhs of Eq. (20) contains a sum over many terms, each one containing the product $B^s B^{s'}$ of two Gaussian-distributed random variables, we conclude that the reduced form factors also have a Gaussian distribution. From Eqs. (12) it follows immediately that for $s \neq s'$, the mean value of the form factor is zero, and it remains to calculate the second moment, see Eq. (13). Inserting Eq. (20) into the left hand side of Eq. (3), and using Eqs. (12), (13), we find

$$\begin{aligned} \langle (sI || V_L(R) Y_L || s'I') (s'I' || V_{L'}(R') Y_{L'} || s''I'') \rangle_{\text{ave}} \\ &= \sum_{N\gamma Jnljn'l'j'} \delta_{ss''} \delta_{II''} \langle B_{N\gamma J;nlj}^{sI} |^2 \rangle_{\text{ave}} \langle B_{N\gamma J;n'l'j'}^{s'I'} |^2 \rangle_{\text{ave}} \\ &\times (-)^{1-2J-I-I'} \frac{1}{4\pi} (2l+1)(2l'+1)(2j+1)(2j'+1)(2I+1)(2I'+1) [(2L+1)(2L'+1)]^{1/2} \\ &\times \begin{pmatrix} l & L & l' \\ 0 & 0 & 0 \end{pmatrix} \begin{pmatrix} l' & L' & l \\ 0 & 0 & 0 \end{pmatrix} \begin{Bmatrix} l & j & \frac{1}{2} \\ j' & l' & L \end{Bmatrix} \begin{Bmatrix} l' & j' & \frac{1}{2} \\ j & l & L' \end{Bmatrix} \begin{Bmatrix} L & j' & j \\ J & I & I' \end{Bmatrix} \begin{Bmatrix} L' & j & j' \\ J & I' & I \end{Bmatrix} \\ &\times (R_{nl} | V_L^{\text{s.p.}}[R] | R_{n'l'}) (R_{n'l'} | V_{L'}^{\text{s.p.}}[R'] | R_{nl}). \quad (21) \end{aligned}$$

The radial form factors depend on R and R' , respectively, as indicated by the arguments of $V_L^{\text{s.p.}}$ and $V_{L'}^{\text{s.p.}}$. In order to perform the summation over N and γ , we use Eq. (18). Changing the summation over γ into an integration, carrying out the summation over N and using the relation

$$\rho_I(\epsilon) = (2I+1)\rho_0(\epsilon) \quad (22)$$

which is valid for levels not too close to the yrast line, we find

$$\sum_{N\gamma} \langle |B_{N\gamma J; nlj}^{sI}|^2 \rangle_{\text{ave}} \langle |B_{N\gamma J; n'l'j'}^{s'I'}|^2 \rangle_{\text{ave}} = (2J+1)(2I+1)^{-1}(2I'+1)^{-1} D_0^A(\epsilon_s) D_0^A(\epsilon_{s'}) \times \int d\epsilon_\gamma \frac{[\Gamma/(2\pi)]^2 \rho_0^{A-1}(\epsilon_\gamma)}{[(\epsilon_s - \bar{\epsilon}_{nl} - \epsilon_\gamma)^2 + \frac{1}{4}\Gamma^2][(\epsilon_{s'} - \bar{\epsilon}_{n'l'} - \epsilon_\gamma)^2 + \frac{1}{4}\Gamma^2]}. \quad (23)$$

Keeping in mind the remarks made in the paragraph preceding Eq. (18), we can roughly evaluate the integral in Eq. (23) as follows. Since ρ_0^{A-1} increases exponentially with ϵ_γ , and since the Lorentzians confine ϵ_γ to values roughly given by $\epsilon_s - \bar{\epsilon}_{nl} \pm \frac{1}{2}\Gamma$ and $\epsilon_{s'} - \bar{\epsilon}_{n'l'} \pm \frac{1}{2}\Gamma$, we obtain the biggest contribution if $\bar{\epsilon}_{nl}$ and $\bar{\epsilon}_{n'l'}$ differ from zero by less than $\approx \frac{1}{2}\Gamma$. Keeping in mind that $\Gamma \approx 5$ to 10 MeV, we therefore confine the summation over (n, l, j) and (n', l', j') in Eq. (21) to the two shells adjacent to the Fermi surface (this restricted summation will be indicated by a prime on the summation symbol), and put $\bar{\epsilon}_{nl} = 0 = \bar{\epsilon}_{n'l'}$ in Eq. (23). We now observe that the product of the two Lorentzians is peaked at $\frac{1}{2}(\epsilon_s + \epsilon_{s'})$ and accordingly replace $\rho_0^{A-1}(\epsilon_\gamma)$ by $\rho_0^{A-1}[\frac{1}{2}(\epsilon_s + \epsilon_{s'})] \cong [\rho_0^{A-1}(\epsilon_s)\rho_0^{A-1}(\epsilon_{s'})]^{1/2}$. Using standard level-density formulas, we can convince ourselves that the last formula is a good approximation for $|\epsilon_s - \epsilon_{s'}| \lesssim \Gamma \lesssim 10$ MeV. The integral over the two Lorentzians can easily be carried out. Replacing $D_0^A(\epsilon_s)[\rho_0^{A-1}(\epsilon_s)]^{1/2}$ by $[D_0^A(\epsilon_s)]^{1/2}$ (which is again a good approximation for heavy nuclei), we find for the rhs of Eq. (23)

the value

$$(2J+1)(2I+1)^{-1}(2I'+1)^{-1} [D_0^A(\epsilon_s)D_0^A(\epsilon_{s'})]^{1/2} \times \frac{\Gamma/(2\pi)}{(\epsilon_s - \epsilon_{s'})^2 + \frac{1}{4}\Gamma^2}. \quad (24)$$

Using this result in Eq. (21), which carries now the restricted summation over (nlj) and $(n'l'j')$ referred to above, we can perform the summations over $J, j,$ and j' . We use the facts that $(I + \frac{1}{2} + J)$ is integer, that we disregard the spin-orbit splitting, and the identities

$$\sum_J (2J+1)(2L+1) \begin{Bmatrix} j & j' & L \\ I' & I & J \end{Bmatrix} \begin{Bmatrix} I' & j' & J \\ j & I & L' \end{Bmatrix} = \delta_{LL'},$$

$$\sum_{j'} (2j'+1)(2l+1) \begin{Bmatrix} l' & L & l \\ j & \frac{1}{2} & j' \end{Bmatrix} \begin{Bmatrix} j & L & j' \\ l' & \frac{1}{2} & l \end{Bmatrix} = 1, \quad (25)$$

$$\sum_j (2j+1) = 2(2l+1).$$

This yields

$$\langle (sI \| V_L(R)Y_L \| s'I')(s'I' \| V_{L'}(R') \| s''I'') \rangle_{\text{ave}} = \delta_{ss''} \delta_{II''} \delta_{LL'} (-1)^{I-I'} [D_0^A(\epsilon_s)D_0^A(\epsilon_{s'})]^{1/2} \frac{\Gamma/(2\pi)}{(\epsilon_s - \epsilon_{s'})^2 + \frac{1}{4}\Gamma^2} \times \sum_{nln'l'}' 2 \frac{(2l+1)(2l'+1)}{4\pi} \begin{pmatrix} l & L & l' \\ 0 & 0 & 0 \end{pmatrix}^2 (R_{nl} | V_L^{s.p.}[R] | R_{n'l'}) (R_{n'l'} | V_{L'}^{s.p.}[R'] | R_{nl}). \quad (26)$$

We compare this result with Eqs. (3) and (4). Recalling Eq. (22), and defining α by analogy to Eq. (3), we find

$$\alpha_L^{\text{theor}}(s, s'; I, I'; R, R') = \frac{\Gamma/(2\pi)}{(\epsilon_s - \epsilon_{s'})^2 + \frac{1}{4}\Gamma^2} [\rho_I(\epsilon_s)\rho_{I'}(\epsilon_{s'})]^{-1/2} \times \sum_{nln'l'}' 2 \frac{(2l+1)(2l'+1)}{2L+1} \begin{pmatrix} l & L & l' \\ 0 & 0 & 0 \end{pmatrix}^2 \times (R_{nl} | V_L^{s.p.}[R] | R_{n'l'}) (R_{n'l'} | V_{L'}^{s.p.}[R'] | R_{nl}). \quad (27)$$

In writing Eq. (27), we have added a superscript "theor" to α to distinguish it from the quantity appearing in Eq. (3). We have also disregarded the difference in level densities between fragment 1 and the full system, cf. the first paragraph of this section.

Comparing Eq. (27) with Eq. (4), we observe that the Lorentzian appearing in the former is re-

placed in the latter by a Gaussian. In view of the stipulations introduced on the behavior of the Lorentzian and the approximations made in deriving Eq. (27), it is, indeed, meaningful to make such a replacement, writing

$$\frac{\frac{1}{4}\Gamma^2}{\epsilon^2 + \frac{1}{4}\Gamma^2} \rightarrow \exp[-\epsilon^2/(2\Gamma^2)]. \quad (28)$$

The two functions appearing in (28) have the same value at $\epsilon=0$ and, within a factor 1.6, the same normalization. After the substitution (28) has been made in Eq. (27), the comparison with Eq. (4) shows that

$$\begin{aligned} \omega_L \exp[-(R-R')^2/(2\sigma^2)] f(\frac{1}{2}(R+R')) \\ \rightarrow 4/(\Gamma\pi) \sum_{nl n'l'} \frac{(2l+1)(2l'+1)}{2L+1} \begin{pmatrix} l & L & l' \\ 0 & 0 & 0 \end{pmatrix}^2 \\ \times (R_{nl} | V_L^{s.p.} [R] | R_{n'l'}) \\ \times (R_{n'l'} | V_L^{s.p.} [R'] | R_{nl}). \end{aligned} \quad (29)$$

It remains to show that the rhs of expression (29) does, indeed, have the factorization property and Gaussian behavior postulated by the lhs, and to determine the values of correlation length σ and strength ω_L . This is the task of numerical calculations described in the next section. From the derivation presented in the present section, it should be clear that ω_L cannot be determined very accurately.

III. DESCRIPTION OF THE CALCULATION

The dependence of the second moment, Eq. (26), on R and R' is found by numerical calculation. Let

$$\begin{aligned} h_L(R, R') = \sum_{nl n'l'} \frac{(2l+1)(2l'+1)}{(2L+1)} \begin{pmatrix} l & L & l' \\ 0 & 0 & 0 \end{pmatrix}^2 \\ \times (R_{nl} | V_L^{s.p.} [R] | R_{n'l'}) \\ \times (R_{n'l'} | V_L^{s.p.} [R'] | R_{nl}). \end{aligned} \quad (30)$$

We evaluate the expression (30) and the radial form factors

$$(R_{nl} | V_L^{s.p.} [R] | R_{n'l'}) = \int_0^\infty dr R_{nl}(r) V_L^{s.p.}(R, r) R_{n'l'}(r) \quad (31)$$

for the reaction $^{40}\text{Ar} + ^{208}\text{Pb}$. Here, R_{nl} is the radial part of a single-particle wave function $\varphi_{nl}^m = r^{-1} R_{nl}(r) Y_l^m$ in ^{208}Pb , and $V_L^{s.p.}(R, r)$ is defined by Eqs. (5) and (6) through the expansion of the mean single-particle potential of the nucleons in ^{40}Ar acting on the nucleons in ^{208}Pb .

The potential $V^{s.p.}(|\vec{R}-\vec{r}|)$ in Eq. (5) was taken to be of Woods-Saxon form,

$$V^{s.p.}(\zeta) = V_0 \left[1 + \exp\left(\frac{\zeta-c}{a}\right) \right]^{-1}, \quad (32)$$

where $\zeta = |\vec{R}-\vec{r}|$. We have taken the values

$$\begin{aligned} V_0 &= 50 \text{ MeV}, \\ c &= 4.5 \text{ fm}, \\ a &= 0.65 \text{ fm}, \end{aligned} \quad (33)$$

which yield a root-mean-square (rms) radius of 4.24 fm. In order to carry out the expansion (6), we approximate $V^{s.p.}(\zeta)$ by a sum of Gaussians,

$$V^{s.p.}(\zeta) \cong V_0 \sum_m v_m \exp(-\lambda_m \zeta^2). \quad (34)$$

Each Gaussian is written in the form

$$\begin{aligned} \exp(-\lambda_m |\vec{R}-\vec{r}|^2) = \exp(-\lambda_m [R^2 + r^2]) \\ \times \exp(2\lambda_m Rr \cos\theta), \end{aligned} \quad (35)$$

and the last factor is expanded⁴ as

$$\exp(z \cos\theta) = \sum_{L=0}^{\infty} (2L+1) F_L(z) P_L(\cos\theta), \quad (36)$$

$$F_L(z) = [\pi/(2z)]^{1/2} I_{L+1/2}(z).$$

The functions $I_{L+1/2}(z)$ are modified spherical Bessel functions of the third order. The functions $F_L(z)$ can be calculated using

$$F_0(z) = \frac{\sinh z}{z}, \quad F_1(z) = (z \cosh z - \sinh z)/z^2, \quad (37a)$$

and the recurrence relation

$$F_{L-1}(z) - F_{L+1}(z) = \frac{2L+1}{z} F_L(z). \quad (37b)$$

If $z \lesssim L$, numerical stability requires that we solve Eq. (37b) in the direction of decreasing L . Using Eqs. (35) and (36) in Eq. (34) and comparing the latter with Eq. (6), we obtain

$$\begin{aligned} V_L^{s.p.}(R, r) = V_0 \sum_m v_m \exp(-\lambda_m [R^2 + r^2]) (2L+1) \\ \times F_L(2\lambda_m Rr). \end{aligned} \quad (38)$$

Figure 3 shows the quality of the Gaussian approximation, Eq. (34). The solid line gives the Woods-Saxon factor, the long-dashed line the function obtained by retaining a single Gaussian in the sum (34), and the short-dashed line the two-Gaussian approximation. The parameters $(\lambda_m v_m)$ of the Gaussians were obtained by minimizing the volume integral of the square of the difference between the potentials (32) and (34), keeping the rms radius at a reasonable value. This yields $v_1 = 1.735$ and $\lambda = 0.073 \text{ fm}^{-2}$ for the single-Gaussian approximation (rms radius 4.55 fm). For the two-Gaussian approximation, we demanded $\lambda_2 = 2\lambda_1$ to avoid numerical instability and obtained $\lambda_1 = 0.095 \text{ fm}^{-2}$, $v_1 = 3.486$, and $v_2 = -2.739$ (rms radius 4.34 fm). Figure 3 shows that the single-Gaussian approximation is fairly good in the surface, but deviates from the Woods-Saxon form in the internal region, while the two-Gaussian approximation is better nearly everywhere. Deeply inelastic collisions take place mainly in the nuclear surface region. We therefore expect the two-Gaussian approximation to be good enough for our purposes. This

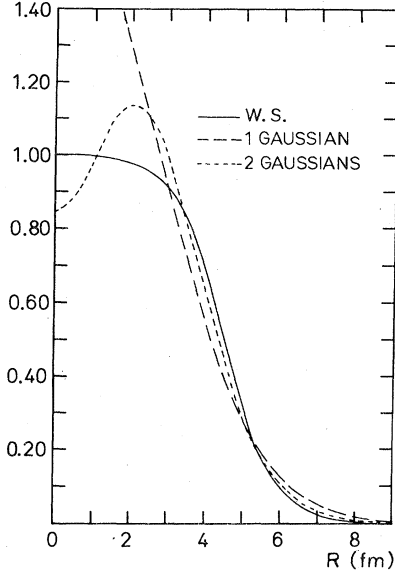


FIG. 3. The Woods-Saxon form factor (solid line), the single-Gaussian approximation (long dashes), and the two-Gaussian approximation (short dashes) plotted versus R (in fm).

will be tested explicitly by comparing the results obtained for the second moment from the single-Gaussian and the two-Gaussian approximations. For those values of R and R' where both approximations give nearly identical results, we can be sure that the internal region is unimportant, and that the approximation in the surface region is sufficiently accurate.

The radial wave functions R_{nl} needed to calculate the expressions (31) were found by numerical integration of the appropriate single-particle Schrödinger equation for ^{208}Pb . For the potential well, we used the Woods-Saxon form (32) with

$$V_0 = -46.2 \text{ MeV}, \quad c = 7.36 \text{ fm}, \quad a = 0.66 \text{ fm} \quad \text{for neutrons;} \\ V_0 = -60.7 \text{ MeV}, \quad c = 7.52 \text{ fm}, \quad a = 0.80 \text{ fm} \quad \text{for protons.}$$

For the protons, we included the Coulomb potential obtained from a uniform charge density distribution which corresponds to the experimentally determined charge rms radius of 5.5 fm. The orbits involved in the restricted summation appearing in Eq. (30) and the associated single-particle separation energies are given in Table I.

The function $h_L(R, R')$ was obtained by numerical integration of the expressions (31), and by numerical summation of the expression (30). Since in Eq. (30) we have $l+L+l'=\text{even}$, the sum in (30) is restricted, for L odd, to matrix elements for the

particle-hole type (excitation across the Fermi surface), for both protons and neutrons. For L even, on the other hand, we get contributions from the hole-hole and from the particle-particle matrix elements, for both protons and neutrons. To account for the proper occupation probability of the hole and the particle orbits, the results for even L were divided by 2. This yielded reasonable agreement with the odd L values.

In order to compare $h_L(R, R')$ with the AKW ansatz (4) we write $h_L(R, R')$ in the form

$$h_L(R, R') = f'_L(\frac{1}{2}(R+R')) g_L(R-R') \quad \text{with } g_L(0) = 1 \quad (40)$$

and ask whether this ansatz can approximately describe our numerical results. In Fig. 4, we show the functions $f'_L(R) = h_L(R, R)$ versus R , for $L=0$ to $L=6$, and for $R > 8$ fm, as obtained from the two-Gaussian approximation. In Fig. 5 we show the function $g_L(R-R') = h_L(R, R') / f'_L(\frac{1}{2}(R+R'))$ for $L=1$, and for the following values of $\frac{1}{2}(R+R') = \bar{R} : \bar{R} = 8 \text{ fm}, \bar{R} = 12 \text{ fm}, \bar{R} = 16 \text{ fm}$. (Note that the quantity \bar{R} is simply denoted by R in Fig. 5.) Figure 6 gives a similar plot for $L=4$. Figure 7 shows g_L at a fixed value of $\bar{R} = 10 \text{ fm}$, and for $L=0$ (full curve) and $L=5$ (dashed-dotted curve). For comparison, the dashed curve is a Gaussian, $\exp[-(R-R')^2/(2\sigma^2)]$, with $\sigma = 3.5 \text{ fm}$.

Figures 5-7 show that in the region of interest, namely $10 \text{ fm} \approx \bar{R} \approx 14 \text{ fm}$, the approximation (40) is quite good, g_L is very close to a Gaussian, and fairly independent of the value of \bar{R} . It is, for $0 \leq L \leq 5$, also fairly independent of L . This justifies the Gaussian ansatz $\exp[-(R-R')^2/(2\sigma^2)]$ in Eq. (4) and suggests for σ a value of about 3.5 fm, independent of L and \bar{R} . Figures 5 and 6 show that for $\bar{R} = 16 \text{ fm}$, a larger value of σ is required. However, such large distances do not play any role in the deeply inelastic collisions.

The function $f(\frac{1}{2}(R+R'))$ introduced in Eq. (4) is related to the function $f'_L(\frac{1}{2}(R+R'))$ defined in Eq. (40) and displayed in Fig. 4 by the relation

$$\omega_L f(\frac{1}{2}(R+R')) = 4/(\pi\Gamma) f'_L(\frac{1}{2}(R+R')). \quad (41)$$

TABLE I. Single-particle orbits and their calculated separation energies (MeV) in ^{208}Pb .

Neutrons		Protons	
0h	13.65	0g	13.58
1f	9.88	1d	9.69
2p	8.35	2s	8.23
0i	6.22	0h	6.78
1g	2.61	1f	2.64
2d	1.52	2p	0.79
3s	1.38		

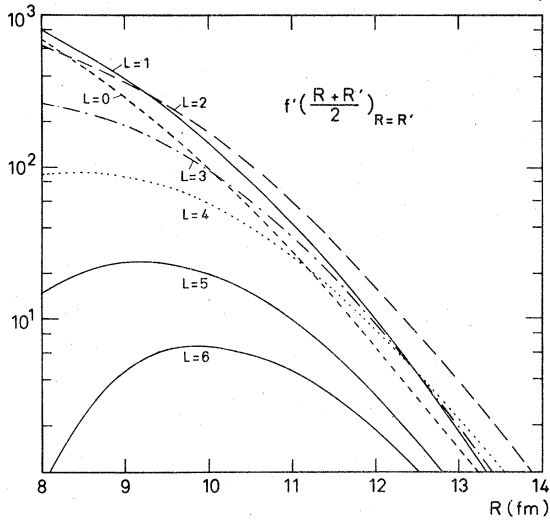


FIG. 4. The function f'_L of Eq. (40) in units MeV^2 plotted versus $\bar{R} = \frac{1}{2}(R+R')$ (in fm) for various L values.

This follows from the relations (29), (30), and (40). Figure 4 shows that for $\bar{R} \geq 10$ fm, all the functions f'_L have roughly the same exponential dependence on \bar{R} , so that Eq. (41) is fulfilled and can be used to determine ω_L . We do this by putting arbitrarily $f(10 \text{ fm}) = 1$ and by choosing $\pi\Gamma/4 = 5$ MeV. (It was emphasized above that this choice of Γ is a rough figure which could equally well be taken to be 10 MeV.) This yields the values for ω_L listed in Table II.

We have checked the accuracy of our numerical results in two ways. We have changed the distance between mesh points in the integration procedure from 0.1 to 0.4 fm, and the results changed insignificantly. We also compared the results of the single-Gaussian approximation with those of the two-Gaussian approximation presented above. The

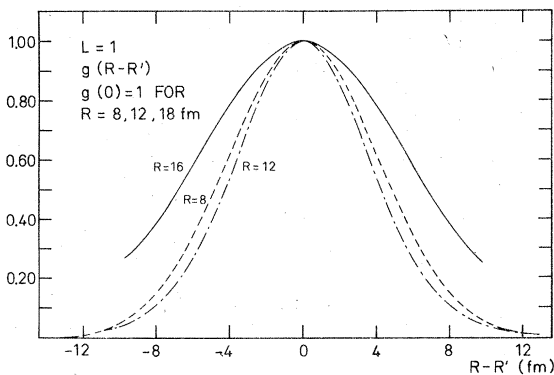


FIG. 5. The function $g_L(R-R')$ of Eq. (40) plotted versus $R-R'$ (in fm) for $L=1$ and for various values of $\bar{R} = \frac{1}{2}(R+R')$. In the figure, \bar{R} is replaced by R .

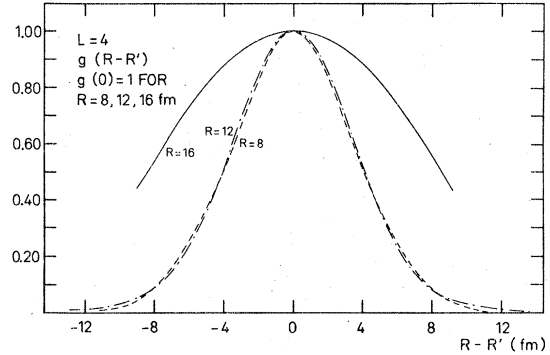


FIG. 6. Same as in Fig. 5 except that $L=4$.

results were very similar for $\bar{R} \geq 10$ fm; significant deviations appeared only for $\bar{R} < 9$ fm. This is the domain for which the density overlap between the two fragments is very considerable; the AKW model which is based on peripheral collisions is not expected to work in this domain. We conclude that for $\bar{R} \geq 10$ fm, our numerical findings are accurate, and that it is only the surface region of the single-particle potential which is important in this domain. For $\bar{R} < 9$ fm, the function f'_L oscillates, for $L \geq 4$, in the two-Gaussian approximation and fails to do so in the single-Gaussian approximation. This shows that in the domain $\bar{R} < 9$ fm, the internal part of the single-particle potential does play an important role.

IV. DISCUSSION OF RESULTS

For the special case of inelastic excitation of nucleons in one fragment by the mean potential of the other, the present study provides a very strong corroboration for the AKW model. The theoretical deliberations of Sec. II have shown that the reduced form factors have a Gaussian distribution with zero

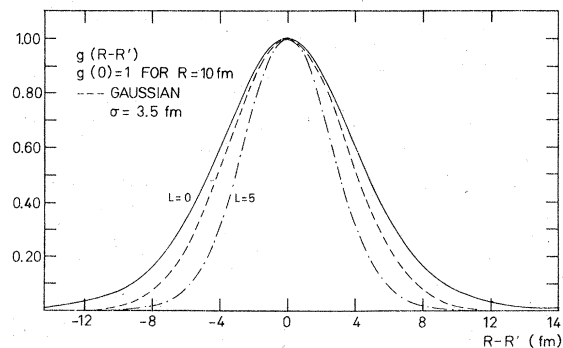


FIG. 7. The function $g_L(R-R')$ of Eq. (40) plotted versus $R-R'$ (in fm) for $L=0$ (full curve) and $L=5$ (dot-long-dashed curve) for $\bar{R} = \frac{1}{2}(R+R') = 10$ fm. The short-dashed curve shows a Gaussian with $\sigma = 3.5$ fm.

TABLE II. The strength factor ω_L as a function of L .

L	ω_L^a (MeV)
0	20.0
1	29.0
2	34.0
3	19.0
4	16.0
5	4.0
6	1.5

^aAs given by Eq. (41) with $f(\frac{1}{2}(R+R'))=1$ at $\frac{1}{2}(R+R')=10$ fm and $\frac{1}{4}(\pi\Gamma)=5$ MeV.

mean. Moreover, the second moment has a value consistent with the ansatz (3), (4). We have seen how the factor involving the level densities in Eq. (4) comes about, and we have indicated the existence of a cutoff factor in energy. It is difficult to ascertain whether this factor is Gaussian in shape, as assumed in Eq. (4). It is equally difficult to give a reliable estimate of the parameter Δ which must be identified with the spreading width Γ , and thus has roughly the value 5 to 10 MeV. It was also pointed out in Sec. II that the overall strength of the second moment cannot be estimated very reliably.

Results of a more definite quantitative nature were obtained on the ratios of the strength factors ω_L , on the form of the function $f(\frac{1}{2}(R+R'))$, on the form of the correlation function in $(R-R')$ which turned out to be Gaussian, and on the correlation length σ . The AKW model is expected to work for c.m. distances $\bar{R}=\frac{1}{2}(R+R')\geq 10$ fm. Indeed, for Ar and Pb the "touching distance," defined by the sum of the two radii taken at the half densities, is about 11 fm. For $\bar{R}\approx 10$ fm, the density overlap of the two fragments is so strong that it is no longer meaningful to talk about separated fragments, and to use an expansion in terms of eigenfunctions of the two separated fragments, as is done in the AKW theory. The results of Fig. 4 show, on the other hand, that for $\bar{R}\geq 15$ fm the mutual overlap has decreased to such a point that nuclear interactions are no longer important and are completely dominated by the Coulomb interaction.

In the domain $10\text{ fm}\leq\bar{R}\leq 15\text{ fm}$, only a few L

values with $L\leq 6$ contribute. The strengths ω_L of the various contributions are listed in Table II. The ratios $\omega_L/\omega_{L'}$ are expected to be determined quite accurately. Higher values of L are unimportant since they give $\omega_L < 1$ MeV. For $L\leq 4$, the strengths ω_L are grouped together quite closely. The function $f(\frac{1}{2}(R+R'))$ is normalized to unity at $\bar{R}=\frac{1}{2}(R+R')=10$ fm and decays exponentially with increasing \bar{R} , see Fig. 4. We have also seen that the correlation function can be approximated surprisingly well by a Gaussian, and that the correlation length σ has approximately the value $\sigma=(3.5\pm 0.7)$ fm, independent of L for $L\leq 5$ and of \bar{R} for $10\text{ fm}\leq\bar{R}\leq 14\text{ fm}$. This value of σ is consistent with the original AKW estimate which stated $\sigma=1$ to 2 fm in the nuclear interior, and somewhat larger in the nuclear surface. Actually, σ has a tendency to increase with \bar{R} and to decrease with L . Both these features can be safely neglected in the domain just indicated.

To test the dependence of our results on mass numbers we performed a similar calculation for Sn (rather than Pb) as the heavy fragment. Our results are in very close agreement with those presented above for Pb. The important L values are restricted to $L\leq 4$ rather than $L\leq 6$ but otherwise nothing changes. This shows that the parametrization (4) should be applicable for all heavy-ion reactions.

The microscope model for form factors of inelastic nucleon scattering developed in the present paper thus produces results consistent with the statistical ansatz of AKW, in the domain of \bar{R} values typical of peripheral collisions, and thus justifies this ansatz microscopically. By giving precise estimates for the correlation length σ , the form of the function $f(\frac{1}{2}(R+R'))$, and the relative importance of various L contributions, the present study narrows down some of the ambiguities of the AKW parametrization. This should help in testing the AKW model by comparing its predictions with the data. Aside from inelastic nucleon scattering, the AKW model also includes nucleon exchange as a mechanism to produce deeply inelastic collisions. An extension of the present study to nucleon transfer processes would therefore be highly desirable.

*Alexander von Humboldt Fellow 1976-77. Permanent address: Department of Physics, University of Arizona, Tucson, Arizona 85721.

†Work supported in part by the NSF (Grant MPS 75-07320).

‡Supported by the Minerva Foundation.

¹D. Agassi, C. M. Ko, and H. A. Weidenmüller, *Ann. Phys. (N.Y.)* **107**, 140 (1977).

²H. A. Weidenmüller, Invited Paper at the Conference

on Heavy Ions, Fall Creek Falls State Park, June, 1977 (to be published), p. 199; D. Agassi, C. M. Ko, and H. A. Weidenmüller.

³C. E. Porter, *Statistical Theory of Spectra-Fluctuations* (Academic, New York, 1965); *Statistical Properties*, edited by J. B. Garg (Plenum, New York, 1972).

⁴M. Abramowitz and I. Stegun, *Handbook of Mathematical Functions* (Dover, New York, 1965), p. 443.